ELSEVIER

Surface Science 433–435 (1999) 506–511

surface science

www.elsevier.nl/locate/susc

Thermal vibrations of a two-dimensional vacancy island crystal in a strained metal film

K. Pohl *, J. de la Figuera, M.C. Bartelt, N.C. Bartelt, J. Hrbek [1], R.Q. Hwang

Sandia National Laboratories, Livermore, CA 94550, USA

Abstract

Vacancy islands formed during room-temperature exposure to sulfur of a submonolayer Ag film on Ru(0001) order spontaneously to form a triangular lattice at an island area fraction just above 20%. A normal mode decomposition of the thermal vibrations of this vacancy island crystal, measured with time-resolved scanning tunneling microscopy, obtains Lamé coefficients in the range of 10^8 N m^{-2}. We show that these estimates are consistent with stabilizing forces derived from long-range elastic interactions between the islands.

Keywords: Lattice vibrations; Nanostructures; Ruthenium; Scanning tunneling microscopy; Self-organization; Silver; Sulfur; Two-dimensional solids

1. Introduction

The spontaneous formation of periodic arrays of voids in the bulk of particle-bombarded materials represents one of the earliest reported observations of self-organized mesoscopic-scale patterns in solids [1,2]. Key processes underlying this periodic ordering remain unsorted, however. Equally fascinating and currently of great technological interest are self-assembled nanometer structures at surfaces, with large-scale order and size uniformity, which are challenging to engineer systematically. The realization that epitaxy on inhomogeneously strained systems, including stepped and anisotropic surfaces, can produce strongly correlated arrays of islands with narrow size and separation distributions, suggested the possibility of creating useful nanoscale structures using standard deposition techniques [3–6]. However, this requires precise control of surface processes over length scales characteristic of strain variations, and the observed degree of order has been consistently inferior to what is typically desired for most applications. Potentially viable alternatives include atomic-scale lithography [7–11], which is still inefficient, and the use of templates, e.g. reconstructed surfaces or lattice mismatched systems, for pre-patterning desired structures [12–16]. In all of these approaches, elastic interactions within the patterned layer are expected to be very important, both in defining its properties and as a fundamental ordering mechanism [17]. What has been missing are direct measurements of such interactions.

Here, we report on a study of the forces responsible for the ordering of a two-dimensional (2D) periodic array of vacancy islands in a strained

* Corresponding author. Fax: +1-925-294-3231.

E-mail address: karsten@io.ca.sandia.gov (K. Pohl)

[1] Permanent address: Brookhaven National Laboratory, Upton, NY 11973, USA.

0039-6028/99/$ – see front matter
PII: S0039-6028(99)00130-2

submonolayer Ag film on Ru(0001), produced during exposure to sulfur at room temperature (RT). Specifically, we analyze thermal vibrations in the array using time-resolved scanning tunneling microscopy (STM), thereby measuring the elastic constants of the array. We propose that the formation of this island crystal can be viewed as the spontaneous formation of a periodic pattern of 2D 'droplets' stabilized by long-range repulsive interactions [18–20]. These droplets (vacancy islands) relax the elastic strain in the (Ag) adlayer, at the cost of creating domain boundaries (island edges). The equilibrium repeat distance and average island size in the pattern reflect the strength of the effective elastic coupling between islands, believed to be a function of the difference in surface stress between the Ag and the surrounding (sulfur-covered) Ru regions [19,20]. We exploit this connection below. Next, we review key experimental details. Our main observations are presented in Section 3. Analysis of the thermal vibrations of the vacancy island crystal is described in Section 4, and estimation of its ordering forces in Section 5.

2. Experimental details

A clean Ru(0001) surface was prepared in ultrahigh vacuum after an initial brief argon sputtering, by repeated oxygen adsorption and flash desorption at 1800 K, and monitored by Auger electron spectroscopy (AES) and a room-temperature STM. Micron-wide terraces, separated by monatomic steps, can be typically obtained on this Ru surface.

Slightly less than one monolayer ($\sim$0.8 ML) of Ag was deposited at RT on the prepared Ru surface by evaporation from a resistively heated tungsten basket, at a rate of $\sim 10^{-2}$ ML s^{-1} as estimated from AES and inspection of STM images. Subsequent flash annealing to 750 K produces a single atomic height film of Ag with the highly ordered equilibrium dislocation pattern shown in Fig. 1a. This structure consists of a network of surface edge dislocations [21,22], which relieve the local strain induced by the 6.6% lattice mismatch between Ag and Ru. In the darker regions in Fig. 1a, Ag atoms reside at bridge sites. These regions nest surface edge dislocations, the cores of which form a near-square array with a unit cell of $\sim 40 \times 60$ Å^2. In the bright regions, the Ag adlayer is pseudomorphic with the Ru substrate, and thus considerably strained. Presumably, both dark and bright regions are locally highly reactive.

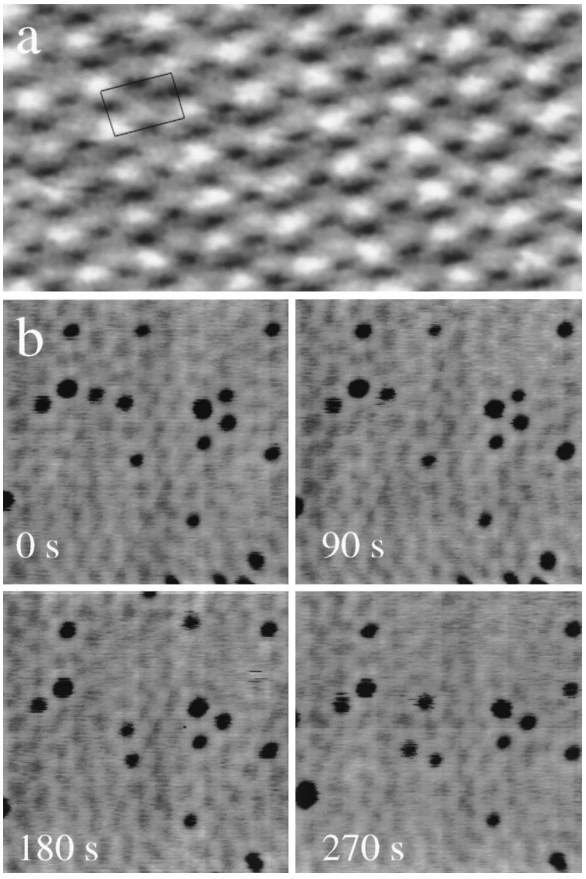

Fig. 1. (a) 400×200 Å^2 STM image of the misfit dislocation structure of the annealed submonolayer Ag/Ru(0001) film. (b) Sequence of STM images, 90 s apart, of the same 500×500 Å^2 area after exposure to 0.04 ML of sulfur at RT. Dark depressions are vacancy islands with a typical density of $\sim 8 \times 10^{-5}$ Å^{-2}.

We exposed this strained Ag film to sulfur at RT. Sulfur is evaporated from an electrochemical doser heated to $\sim$470 K and biased between 0.15 and 2 V [23]. The typical dosing rate was $\sim 5 \times 10^{-3}$ ML s^{-1} at a background pressure of

5×10^{-10} Torr. After sulfur deposition the chamber pressure returned to 5×10^{-11} Torr, and no significant contamination was observed for many hours.

3. Experimental results

3.1. Low sulfur coverage (≤ 0.05 ML)

In the first stages of the reaction, sulfur etches the region around the cores of the dislocations in the Ag film, forming highly mobile vacancy islands of monatomic depth, about 34 Å (± 11 Å) in diameter; see Fig. 1b. While isolated, these islands are observed to move. The islands are significantly more mobile than has been observed for diffusion of homoepitaxial vacancy islands of similar size on metal(111) surfaces [24,25]. From sequences of time-resolved STM images, we measured random net displacements of isolated islands of the order of 65 Å at 48 s intervals. Hopping seems to occur between nearest-neighbor (NN) grid positions defined by the dislocation network, corresponding to an effective island hop rate of $\sim 0.1\ s^{-1}$ at RT. When islands meet they often form stable clusters of two or more islands. In these clusters, the islands are ~ 50 Å apart. These clusters dissociate within a few hundred seconds, as illustrated in Fig. 1b. Strong short-range repulsions between islands in a cluster seem to prevent them from coming close or coalescing. The high mobility of the islands suggests that the surface configuration in Fig. 1b is equilibrated.

Atomic resolution images of the largest islands, and of the Ru regions not covered with Ag, reveal ordered 2D sulfur clusters coating the exposed Ru; see Fig. 2a. The sulfur adatoms form a $p(2 \times 2)$ structure, as observed in previous sulfur-on-Ru(0001) adsorption experiments [26,27]. The surface height profile in Fig. 2b extends across an average-sized vacancy island and a neighboring larger island. While the individual sulfur adatoms covering the larger island (~ 50 Å diam.) are clearly resolved, the presence of sulfur in the smaller island (~ 30 Å diam.) can only be inferred from the fact that the profile shows the same average height inside small and large islands. Also, we note that the sulfur coverage estimated from the area fraction of vacancy islands (assuming they are all coated with sulfur), and the density in a $p(2 \times 2)$ structure, are consistent with sulfur coverages estimated from AES, within the large uncertainty in the AES value due to the complicated surface morphology. The presence of sulfur covering the Ru regions is not surprising because it lowers their surface free energy and forms a strong S–Ru bond [26,27].

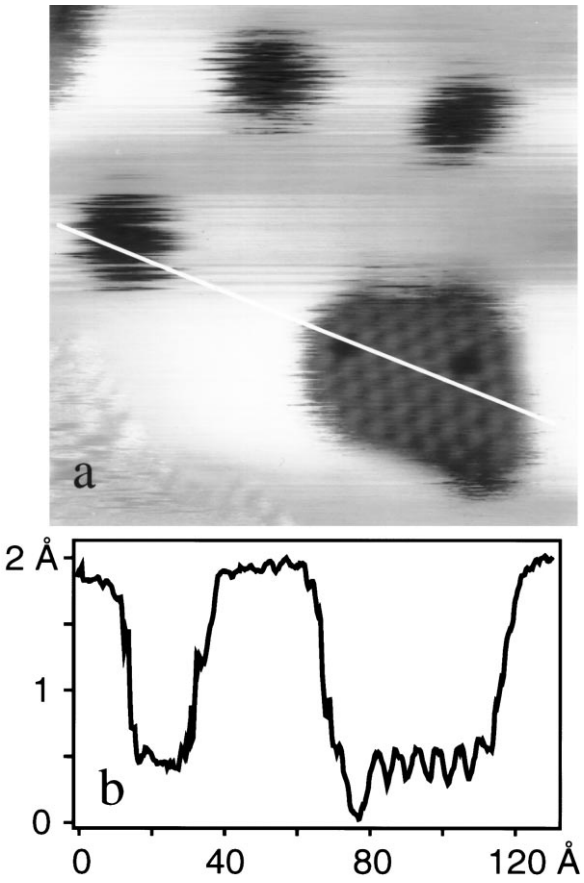

Fig. 2. (a) Atomically resolved STM image (115×115 Å^2) of a large vacancy island, about 50 Å in diameter. The island step edges of this and the smaller islands move much faster than the acquisition rate of the STM images, and thus appear 'blurred'. A cluster of nearly 50 sulfur adatoms inside the large island exhibits $p(2 \times 2)$ order. These large islands are immobile compared with the smaller islands, but 'breathe' on the time scale of STM image acquisition. (b) STM line scan showing the depth of small and large vacancy islands in the Ag adlayer, and atomically-resolved sulfur at the bottom of the large island.

3.2. Higher sulfur coverage ($\sim$0.1 ML)

With increasing sulfur coverage, the densities of vacancy islands, and self-assembled clusters of islands, increase and the average size of individual islands decreases slightly (to $\sim$24 Å average diameter). For sulfur coverages close to 0.1 ML, a highly ordered triangular lattice of vacancy islands forms, with period $b \approx 53$ Å; see Fig. 3. The Fourier transform of this 2D crystal obtains a sharp six-fold diffraction pattern. The distribution of island sizes is also extremely narrow, as shown in Fig. 3c. The width of the distribution of island diameters, ± 4 Å (assuming near-circular islands), is comparable with the imaged width of the island edges. We find a few defects in the crystal, mostly larger vacancy islands ($\sim$50 Å in diameter and density of $\sim 2 \times 10^{-5}$ islands/Å^2), which we observed to form by accretion of two or more individual islands during larger amplitude vibrations. In addition, we find pairs of dislocation lines, with density of $\sim 7 \times 10^{-6}$ lines/Å^2. Fig. 3a and b show a few examples of these defects.

4. Analysis of thermal vibrations in the vacancy island crystal

Thermal vibrations in the lattice of vacancy islands were observed on the time-scale of STM image acquisition, every 20 s. At RT, we measured vibrational amplitudes as large as 10 Å, one fifth of the average separation between NN islands; see Fig. 3d. We followed the motion of the center-of-mass (CM) of each island in a nearly defect-free 450×450 Å^2 array of about 80 islands by time-resolved STM. taking images every 20 s. For quantitative analysis of this motion, gray scale images

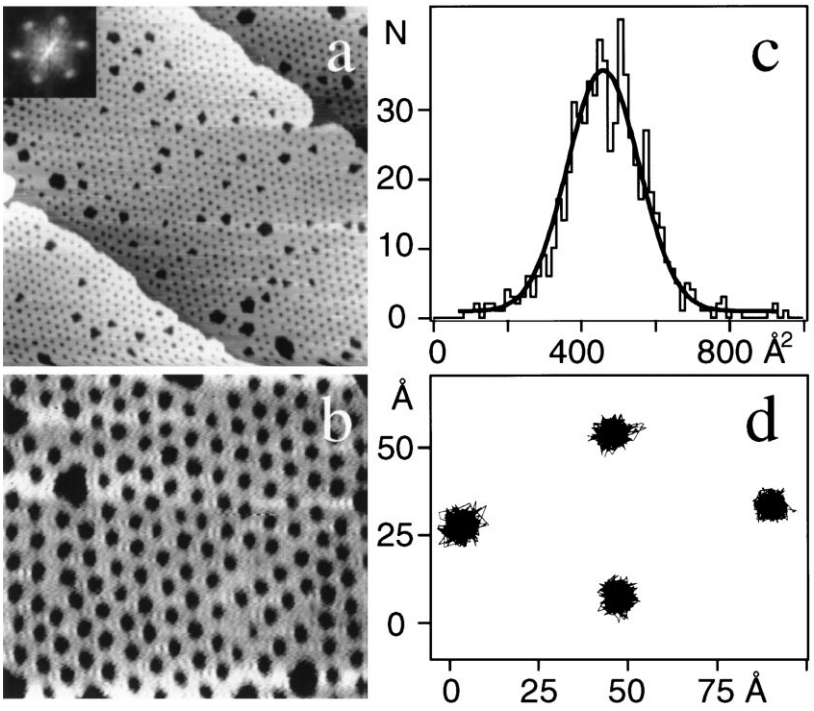

Fig. 3. (a) 2000×2000 Å^2 image of the 2D vacancy island crystal. Three Ru terraces are shown (stepping down from the bottom left to the upper right corner). The inset shows the Fourier transform of the image. (b) A 700×640 Å^2 zoom on the STM image in (a). (c) Size distribution of the vacancy islands: N is the number of islands and the solid line is the Gaussian fit. The average area is $\sim$462 Å^2; the standard deviation is $\sim$117 Å^2. (d) Trajectories of the CM of four NN vacancy islands; the positions are measured every 20 s. Motion of the islands about their equilibrium positions is presumably associated with diffusion of Ag atoms and vacancies along the perimeter and across the interior of the islands.

of 165×165 pixels were then converted into binary black-and-white frames, by thresholding near the midpoint of the intensity histogram of each image. This procedure typically leaves spurious 0 and 1 pixels, which we eliminated using a NN 'majority' rule that conserved the number of vacancies (the fraction of dark pixels per frame) in the sequence of images. Vacancy islands were identified as connected clusters of dark pixels (using NN connectivity), and then consistently labeled for all frames. Finally, the coordinates of the CM of each island were recorded for subsequent analysis of the corresponding displacements along the sequence; cf. Fig. 3d.

We find that the CM motion is correlated for neighboring islands, 'in-phase' motion having higher probability [28]. Since they are small, the CM displacements of the islands can be viewed as 'vibrations in a harmonic crystal' (although inertia plays no role here; the motion of our islands is strictly diffusive). In this case, a simple relation exists between the CM displacement field, $\boldsymbol{u}(\boldsymbol{r}, t) = \boldsymbol{r}(t) - \boldsymbol{r}_0$, for an island of CM coordinate $\boldsymbol{r}(t)$ at time t, and equilibrium CM position $\boldsymbol{r}_0$, and the elastic constants of the island crystal. This relation is especially simple in Fourier space because in a harmonic crystal there is equipartition of energy among the Fourier modes. This equipartition gives an expression for the equilibrium correlation functions $G_{ll} = \langle u^l(q) u^l(-q) \rangle / A = [k_B T/(\mu q^2)][1 - (\mu + \lambda)/(2\mu + \lambda)]$ and $G_{tt} = \langle u^t(q) u^t(-q) \rangle / A = k_B T/(\mu q^2)$ for modes longitudinal (l) and transverse (t) to $\boldsymbol{q}$, respectively, in the long wavelength limit [29,30]. Here, $\langle \ldots \rangle$ denotes an ensemble average, λ and μ are the Lamé constants of the lattice, T is the temperature, k_B is the Boltzmann constant, and A is the system area. Thus, measurement of G_{ll} and G_{tt} for one or more small q values allows determination of λ and μ. For a perfectly ordered 6×6 vacancy island cell, and the smallest non-zero $q = 4\pi/(10\sqrt{3}b) \approx 0.14\ \mathrm{nm}^{-1}$, we estimate $G_{ll} \approx 3 \pm 1\ \mathrm{nm}^4$ and $G_{tt} \approx 4 \pm 2\ \mathrm{nm}^4$, so $\lambda/c \approx \mu/c \approx 10^8\ \mathrm{N\,m}^{-2}$. Here, $c \approx 4$ Å is the vertical lattice spacing of the Ag/Ru(0001) film, and is introduced to facilitate comparison with bulk values (non-withstanding major differences in the physics underlying phonon behavior in a crystal of atoms and thermal fluctuations in our island crystal). Typically, one finds significantly larger values for the bulk quantities, $\lambda_{bulk} \approx 10^{11}\ \mathrm{N\,m}^{-2}$ and $\mu_{bulk} \approx 10^{10}\ \mathrm{N\,m}^{-2}$, reflecting the fact that the long-ranged ordering forces of the vacancy island lattice are much weaker than the forces ordering atomic crystals (which is no surprise!). We believe that the source of the interactions between the vacancy islands is the weak interfering strain fields in the Ru substrate surface around each island, as we discuss in the following section.

5. Connection to the elastic coupling between islands

In order to access the magnitude of the forces stabilizing the array of islands, we consider a simple model which can account for the spontaneous formation of such an array and provide a direct connection between the magnitude of the forces and the elastic constants estimated above [19,20]. The model has two basic ingredients. (1) The line tension γ_b, i.e. the energy per unit length of the vacancy island edges, expressing the cost of reducing the local coordination of edge atoms. It favors the formation of few large islands. For vacancy islands on Ag(111), one has $\gamma_b \approx 0.1\ \mathrm{eV\,Å}^{-1}$ [31]. (2) An effective repulsive interaction, γ_d, between neighboring island edges, driven by elastic relaxations in the Ag adlayer and in the Ru substrate. It favors the formation of many small islands. At low area fraction of single vacancies, the lowest energy structure in this model is a hexagonal crystal of near-circular vacancy islands of sharply distributed radius, R, and repeat distance, b. These predictions agree qualitatively with our observations. For that model, one readily arrives at the relation $\gamma_d = \sqrt{3}(\lambda + \mu) b^2/(\pi R)$. From the measured λ and μ, we obtain $\gamma_d \approx 0.2\ \mathrm{eV\,Å}^{-1}$. This estimate of γ_d can be related directly to the stress field around each island, as determined by the elastic constants of the substrate and the difference in the surface stress between Ag and Ru regions [17,28].

Other predictions from this model [19,20], like the formation of an array of Ag stripes at interme-

diate values of the area fraction of single vacancies, warrant further analysis. Similarly, the atomic processes involved in the displacement of Ag by sulfur, and the possible role of the original dislocation network in the Ag film in the selection of crystal parameters, need detailed examination.

Acknowledgements

This work was supported by the Office of Basic Energy Sciences, Division of Materials Sciences of the US Department of Energy under contract no. DE-AC04-94AL85000 and DE-AC2-98CH 10886. J. de la Figuera acknowledges support from the Fulbright Commission and the Spanish MEC (FU96/2608966).

References

[1] J.H. Evans, Nature 229 (1971) 403.
[2] W. Jäger, H. Trinkaus, J. Nucl. Mater. 205 (1993) 394.
[3] J. de la Figuera, M.A. Huerta-Garnica, J.E. Prieto, C. Ocal, R. Miranda, Appl. Phys. Lett. 66 (1995) 1006.
[4] D.S.L. Mui, D. Leonard, L.A. Coldren, P.M. Petroff, Appl. Phys. Lett. 66 (1995) 1620.
[5] J. Tersoff, C. Teichert, M.G. Lagally, Phys. Rev. Lett. 76 (1996) 1675.
[6] F.J. Himpsel, T. Jung, J.E. Ortega, Surf. Rev. Lett. 4 (1997) 371.
[7] D.M. Eigler, E.K. Schweizer, Nature 344 (1990) 524.
[8] J.A. Stroscio, D.M. Eigler, Science 254 (1991) 1319.
[9] M.F. Crommie, C.P. Lutz, D.M. Eigler, Science 262 (1993) 218.
[10] Ph. Avouris, I.-W. Lyo, R.E. Walkup, Y. Hasegawa, J. Vac. Sci. Technol. B 12 (1994) 1447.
[11] G. Meyer, K.H. Rieder, MRS Bull. 23 (1998) 28.
[12] T.M. Parker, L.K. Wilson, N.G. Gordon, F.M. Leibsle, Phys. Rev. B 56 (1997) 6458.
[13] Ch. Ammer, K. Meinel, H. Wolter, H. Neddermeyer, Surf. Sci. 377–379 (1997) 81.
[14] D.D. Chambliss, R.J. Wilson, S. Chiang, Phys. Rev. Lett. 66 (1991) 1721.
[15] B. Voigtländer, G. Meyer, N.M. Amer, Phys. Rev. B 44 (1991) 10354.
[16] B. Voigtländer, G. Meyer, N.M. Amer, Surf. Sci. 255 (1991) L529.
[17] H. Ibach, Surf. Sci. Rep. 29 (1997) 193.
[18] M. Seul, D. Andelman, Science 267 (1995) 476.
[19] D. Vanderbilt, Surf. Sci. 268 (1992) L300.
[20] K.-O. Ng, D. Vanderbilt, Phys. Rev. B 52 (1995) 2177.
[21] J.L. Stevens, R.Q. Hwang, Phys. Rev. Lett. 74 (1995) 2078.
[22] R.Q. Hwang, J.C. Hamilton, J.L. Stevens, S.M. Foiles, Phys. Rev. Lett. 75 (1995) 4242.
[23] G.-Q. Xu, J. Hrbek, Catal. Lett. 2 (1989) 199.
[24] J. de la Figuera, J.E. Prieto, C. Ocal, R. Miranda, Solid State Commun. 89 (1994) 815.
[25] K. Morgenstern, G. Rosenfeld, B. Poelsema, G. Comsa, Phys. Rev. Lett. 74 (1995) 2058.
[26] R. Dennert, M. Sokolowski, H. Pfnür, Surf. Sci. 271 (1992) 1.
[27] J. Hrbek, A.K. Schmid, M.C. Bartelt, R.Q. Hwang, Surf. Sci. 385 (1997) L1002.
[28] K. Pohl, M.C. Bartelt, J. de la Figuera, N.C. Bartelt, J. Hrbek, R.Q. Hwang, Nature 397 (1999) 238.
[29] D.R. Nelson, B.I. Halperin, Phys. Rev. B 19 (1979) 2457.
[30] D.A. Huse, Phys. Rev. B 28 (1983) 6110.
[31] K. Morgenstern, G. Rosenfeld, G. Comsa, Phys. Rev. Lett. 76 (1996) 2113.